

C₃-Symmetric Trinuclear Molybdenum Cluster Sulfides: Configurational Stability, Supramolecular Stereocontrol, and Absolute Configuration Assignment

Richard Frantz,[†] Eva Guillamón,[‡] Jérôme Lacour,^{*,†} Rosa Llusar,^{*,‡} Victor Polo,[‡] and Cristian Vicent[§]

Département de Chimie Organique, Université de Genève, quai Ernest-Ansermet 30, CH-1211 Genève 4, Switzerland, and Departament de Química Física i Analítica, and Serveis Centrals d'Instrumentació Científica, Universitat Jaume I, Avda. Sos Baynat s/n, E-12080, Castelló, Spain

Received July 31, 2007

The chiral C₃-symmetric [Mo₃S₄Cl₃(dppe)₃]⁺ cluster [dppe = 1,2-bis(diphenylphosphinoethane), *P* or *M* enantiomers] with incomplete cuboidal structure is shown to be configurationally stable at room temperature and configurationally labile at elevated temperature using enantiopure Δ- or Λ-TRISPHAT [(tris(tetrachlorobenzenediolato)phosphate(V)) anions both as chiral NMR solvating and asymmetry-inducing reagents. It is evidenced that the enantiomers of this trinuclear cluster cation can equilibrate at higher temperature (typically 72 °C), and in the presence of the hexacoordinated phosphate anion, a moderate level of stereocontrol (1.2:1) can be achieved. It results in a diastereomeric enrichment of the solution in favor of the heterochiral ion pairs, e.g., *M*⁺ Δ⁻ or *P*⁺ Λ⁻. At higher temperature, a partial racemization of the TRISPHAT anion is also observed, and precipitation at room temperature of [*rac*-Mo₃S₄Cl₃(dppe)₃][*rac*-TRISPHAT] salts from the diastereomeric enriched solution improves the diastereomeric purity of the mother liquor to a 4:1 ratio. A low-energy pathway for the interconversion between the [*P*-Mo₃S₄Cl₃(dppe)₃]⁺ and [*M*-Mo₃S₄Cl₃(dppe)₃]⁺ enantiomers has been found using combined quantum mechanics and molecular mechanics methodologies. This pathway involves two intermediates with three transition state regions, which result from the partial decoordination of the diphosphane coordinated at each metal center. Such decoordination creates a vacant position on the metal, producing a Lewis acidic site that presumably catalyzes the TRISPHAT epimerization.

Introduction

Chiral molecules with only 3-fold rotational axes have been considerably less investigated than their lower rotational symmetry congeners, despite often simple preparative procedures and effective asymmetric properties.¹ In the past years, efficient synthetic strategies were developed for the preparation of racemic C₃-symmetric cluster complexes of the formula [M₃Q₄X₃(diphosphane)₃]⁺ (M = Mo, W; Q = S, Se; X = halide, H, or OH).^{2–4} These cationic complexes possess an incomplete cuboidal structure, with the metal atoms defining an equilateral triangle and one capping and three bridging sulfur atoms. Each of the three metal centers

connected to the diphosphane ligands is stereogenic and a global absolute configuration can be assigned using *P* and *M* descriptors, which refer to the rotation of the X ligands around the C₃ axis, with the capping sulfur atom pointing toward the viewer, as illustrated in Figure 1. In addition, such Mo₃S₄ complexes can act as metalloligands toward a second transition metal M' to afford heterobimetallic catalytically active Mo₃M'S₄ clusters. In particular, [Mo₃CuS₄(diphosphane)₃Cl₄]⁺ cluster complexes are efficient catalysts for the intramolecular cyclopropanation of 1-diazo-5-hexen-2-one and for the intermolecular cyclopropanation of alkenes such as styrene and 2-phenylpropene, with ethyl diazoacetate.⁴

Recently, the stereoselective synthesis of [Mo₃S₄Cl₃(diphosphane)₃]⁺ cationic clusters was tackled using chiral enantiopure diphosphane ligands as chiral auxiliaries. The excision in boiling acetonitrile of the polymeric {Mo₃S₇Cl₄}_{*n*}

* Authors to whom correspondence should be addressed. J.L.: fax, (+41)223792115; e-mail, jerome.lacour@chiorg.unige.ch. R.L.: fax, (+34)-964728066; e-mail, Rosa.Llusar@qfa.uji.es.

[†] Université de Genève.

[‡] Departament de Química Física i Analítica, Universitat Jaume I.

[§] Serveis Centrals d'Instrumentació Científica, Universitat Jaume I.

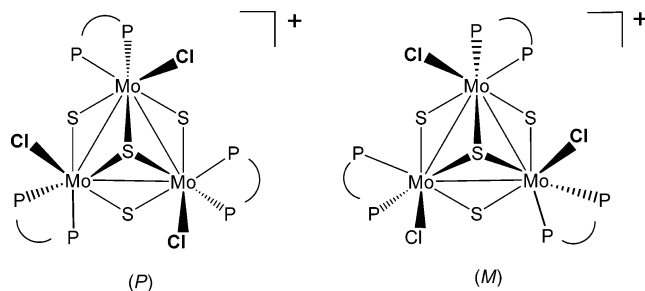


Figure 1. Chiral $[\text{Mo}_3\text{S}_4\text{Cl}_3(\text{diphosphane})_3]^+$ complexes of *P* and *M* configurations.

phase with either (+)-1,2-bis[(2*R*,5*R*)-2,5-(dimethylphospholan-1-yl)ethane [(*R,R*)-Me-BPE] or its enantiomer (*S,S*)-Me-BPE afforded enantiopure (*P*)- and (*M*)- $[\text{Mo}_3\text{S}_4\text{Cl}_3(\text{Me-BPE})_3]^+$ clusters, respectively, as single stereoisomers.⁴ However, the origin of the full stereocontrol was not explained, and three hypotheses could be envisioned to rationalize the result. First, a thermodynamic control in the event of configurationally labile stereoisomers at room temperature; second, kinetic control in the case of configurationally stable entities at room and elevated temperatures; and finally, a combination of the two, i.e., configurational stability at room temperature and lability at ca. 81 °C (boiling point of acetonitrile).⁵ To determine the correct hypothesis among the three, it was decided to attempt the resolution of

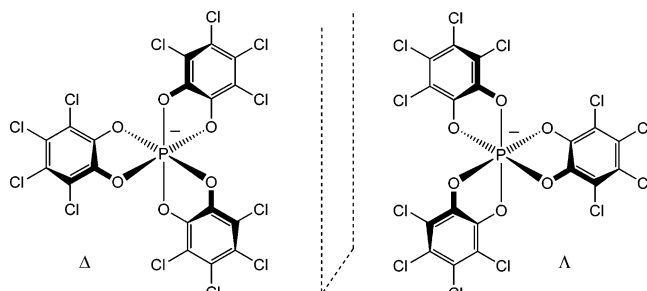


Figure 2. Hexacoordinated phosphate anion TRISPHAT (Δ and Λ enantiomers).

a cluster complex made of achiral diphosphane ligands, the isolation of nonracemic fractions of the cationic complex at room and possibly at elevated temperature being, for instance, a decisive element for the distinction of the three options.

Previously, the hexacoordinated phosphorus anion TRISPHAT [tris(tetrachlorobenzene-1,3,5-triolato)phosphate(V), Δ or Λ enantiomers; Figure 2]^{6,7} has been shown to be an interesting chiral anionic counterion for chiral cationic species.⁸ When associated with configurationally stable cations, it behaves as a NMR chiral solvating and resolving agent.^{9,10} When associated with configurationally labile cations, supramolecular diastereoselective interactions can occur and one diastereomeric ion pair can become predominant in solution; the occurrence of such a behavior (Pfeiffer effect)¹¹ is a good probe of the lack of configurational stability of the cation.^{12–14} The association of Δ - or Λ -TRISPHAT anion with a racemic $[\text{Mo}_3\text{S}_4\text{Cl}_3(\text{diphosphane})_3]^+$ cluster cation was then particularly interest-

- (1) Moberg, C. *Angew. Chem., Int. Ed.* **1998**, *37*, 248–268. Moberg, C. *Angew. Chem., Int. Ed.* **2006**, *45*, 4721–4723. Okamoto, T.; Irie, R.; Katsuki, T. *J. Organomet. Chem.* **2007**, *692*, 645–653. Mba, M.; Prins, L. J.; Licini, G. *Org. Lett.* **2007**, *9*, 21–24. Fabris, F.; Pellizzaro, L.; Zonta, C.; De Lucchi, O. *Eur. J. Org. Chem.* **2007**, 283–291. Bailey, P. J.; McCormack, C.; Parsons, S.; Rudolph, F.; Perucha, A. S.; Wood, P. *Dalton Trans.* **2007**, 476–480. Axe, P.; Bull, S. D.; Davidson, M. G.; Gilfillan, C. J.; Jones, M. D.; Robinson, D.; Turner, L. E.; Mitchell, W. L. *Org. Lett.* **2007**, *9*, 223–226. Wroblewski, A. E.; Halajewski-Wosik, A. *Synthesis* **2006**, 989–994. Sala, X.; Rodriguez, A. M.; Rodriguez, M.; Romero, I.; Parella, T.; von Zelewsky, A.; Llobet, A.; Benet-Buchholz, J. *J. Org. Chem.* **2006**, *71*, 9283–9290. Pei, Y. X.; Brule, E.; Moberg, C. *Org. Biomol. Chem.* **2006**, *4*, 544–550. Fang, T.; Xu, J. X.; Du, D. M. *Synlett* **2006**, 1559–1563. Du, D. M.; Fang, T.; Xu, J. X.; Zhang, S. W. *Org. Lett.* **2006**, *8*, 1327–1330. Ye, M. C.; Li, B.; Zhou, J.; Sun, X. L.; Tang, Y. *J. Org. Chem.* **2005**, *70*, 6108–6110. Ward, B. D.; Bellemin-Lapponnaz, S.; Gade, L. H. *Angew. Chem., Int. Ed.* **2005**, *44*, 1668–1671. Schopohl, M. C.; Faust, A.; Mirk, D.; Frohlich, R.; Kataeva, O.; Waldvogel, S. R. *Eur. J. Org. Chem.* **2005**, 2987–2999. Ionescu, G.; van der Vlugt, J. I.; Abbenhuis, H. C. L.; Vogt, D. *Tetrahedron: Asymmetry* **2005**, *16*, 3970–3975. Haberhauer, G.; Oeser, T.; Rominger, F. *Chem. Commun.* **2005**, 2799–2801. Castaldi, M. P.; Gibson, S. E.; Rudd, M.; White, A. J. P. *Chem. Eur. J.* **2005**, *12*, 138–148. Lam, T. C. H.; Mak, W. L.; Wong, W. L.; Kwong, H. L.; Sung, H. H. Y.; Lo, S. M. F.; Williams, I. D.; Leung, W. H. *Organometallics* **2004**, *23*, 1247–1252 and references therein.
- (2) Feliz, M.; Llusar, R.; Uriel, S.; Vicent, C.; Humphrey, M. G.; Lucas, N. T.; Samoc, M.; Luther-Davies, B. *Inorg. Chim. Acta* **2003**, *349*, 69–77. Estevan, F.; Feliz, M.; Llusar, R.; Mata, J. A.; Uriel, S. *Polyhedron* **2001**, *20*, 527–535.
- (3) Basallote, M. G.; Feliz, M.; Fernandez-Trujillo, M. J.; Llusar, R.; Safont, V. S.; Uriel, S. *Chem. Eur. J.* **2004**, *10*, 1463–1471. Feliz, M.; Llusar, R.; Uriel, S.; Vicent, C.; Coronado, E.; Gomez-Garcia, C. I. *Chem. Eur. J.* **2004**, *10*, 4308–4314. Feliz, M.; Llusar, R.; Uriel, S.; Vicent, C.; Brorson, M.; Herbst, K. *Polyhedron* **2005**, *24*, 1212–1220. Algarra, A. G.; Basallote, M. G.; Castillo, C. E.; Corao, C.; Llusar, R.; Fernandez-Trujillo, M. J.; Vicent, C. *Dalton Trans.* **2006**, 5725–5733.
- (4) Feliz, M.; Guillaumon, E.; Llusar, R.; Vicent, C.; Stiriba, S. E.; Perez-Prieto, J.; Barberis, M. *Chem. Eur. J.* **2006**, *12*, 1486–1492.
- (5) This last possibility allows a thermodynamic “check-up” of the three successive ring-closures at elevated temperatures, leading to a single diastereoisomer, that diastereomer being then completely inert at room temperature.

- (6) Lacour, J.; Ginglinger, C.; Grivet, C.; Bernardinelli, G. *Angew. Chem., Int. Ed.* **1997**, *36*, 608–610.
- (7) Favarger, F.; Goujon-Ginglinger, C.; Monchaud, D.; Lacour, J. *J. Org. Chem.* **2004**, *69*, 8521–8524.
- (8) Lacour, J.; Hebbe-Viton, V. *Chem. Soc. Rev.* **2003**, *32*, 373–382. Constant, S.; Lacour, J. *Top. Curr. Chem.* **2005**, *250*, 1–41. Lacour, J.; Frantz, R. *Org. Biomol. Chem.* **2005**, *3*, 15–19.
- (9) Mimassi, L.; Cordier, C.; Guyard-Duhayon, C.; Mann, B. E.; Amouri, H. *Organometallics* **2007**, *26*, 860–864. Frantz, R.; Grange, C. S.; Al-Rasbi, N. K.; Ward, M. D.; Lacour, J. *Chem. Commun.* **2007**, 1459–1461. Correia, I.; Amouri, H.; Cordier, C. *Organometallics* **2007**, *26*, 1150–1156. Hutin, M.; Frantz, R.; Nitschke, J. R. *Chem. Eur. J.* **2006**, *12*, 4077–4082. Frantz, R.; Pinto, A.; Constant, S.; Bernardinelli, G.; Lacour, J. *Angew. Chem., Int. Ed.* **2005**, *44*, 5060–5064. Mimassi, L.; Guyard-Duhayon, C.; Rager Marie, N.; Amouri, H. *Inorg. Chem.* **2004**, *43*, 6644–6649. Hamelin, O.; Pecaut, J.; Fontecave, M. *Chem. Eur. J.* **2004**, *10*, 2548–2554. Gruselle, M.; Thouvenot, R.; Malezieux, B.; Train, C.; Gredin, P.; Demeschik, T. V.; Troitskaya, L. L.; Sokolov, V. I. *Chem. Eur. J.* **2004**, *10*, 4763–4769. Djukic, J.-P.; Berger, A.; Pfeffer, M.; de Cian, A.; Kyritsakas-Gruber, N.; Vachon, J.; Lacour, J. *Organometallics* **2004**, *23*, 5757–5767. Bark, T.; von Zelewsky, A.; Rappoport, D.; Neuburger, M.; Schaffner, S.; Lacour, J.; Jodry, J. *J. Chem. Eur. J.* **2004**, *10*, 4839–4845. Chavarot, M.; Menage, S.; Hamelin, O.; Charnay, F.; Pecaut, J.; Fontecave, M. *Inorg. Chem.* **2003**, *42*, 4810–4816. Planas, J. G.; Prim, D.; Rose-Munch, F.; Rose, E.; Thouvenot, R.; Vaissermann, J. *Organometallics* **2002**, *21*, 4385–4389. Amouri, H.; Thouvenot, R.; Gruselle, M. C. R. *Chim.* **2002**, *5*, 257–262. Monchaud, D.; Lacour, J.; Coudret, C.; Frayssé, S. *J. Organomet. Chem.* **2001**, *624*, 388–391. Giner Planas, J.; Prim, D.; Rose-Munch, F.; Rose, E.; Monchaud, D.; Lacour, J. *Organometallics* **2001**, *20*, 4107–4110. Ratni, H.; Jodry, J. J.; Lacour, J.; Kündig, E. P. *Organometallics* **2000**, *19*, 3997–3999. Lacour, J.; Goujon-Ginglinger, C.; Torche-Haldimann, S.; Jodry, J. J. *Angew. Chem., Int. Ed.* **2000**, *39*, 3695–3697. Jodry, J. J.; Lacour, J. *Chem. Eur. J.* **2000**, *6*, 4297–4304.
- (10) Ginglinger, C.; Jeannerat, D.; Lacour, J.; Jugé, S.; Uziel, J. *Tetrahedron Lett.* **1998**, *39*, 7495–7498.

ing, as the observation of stereocontrol over the configuration of the cationic complex by the anion would simply and directly demonstrate the occurrence of a configurational lability of the Mo₃S₄ cluster at a given temperature. Herein, using this method, we report that cluster [Mo₃S₄Cl₃(dppe)₃]⁺ [dppe = bis(diphenylphosphinoethane)] is configurationally stable at room temperature and labile at 72 °C. Theoretical investigations aimed at determining a feasible mechanism for the interconversion between the *P* and *M* configurations in these cluster complexes are also presented.

Results and Discussion

Association of Racemic [Mo₃S₄Cl₃(dppe)₃]⁺ with Δ-TRISPHAT. The first step of this work was thus to associate enantiopure TRISPHAT anions with a racemic cluster cation made of achiral diphosphane ligands. Complex [Mo₃S₄Cl₃(dppe)₃]⁺ was selected for its ease of synthesis and structural analogy with previously reported nonracemic structures.⁴ The salt [*rac*-Mo₃S₄Cl₃(dppe)₃][Δ-TRISPHAT] was prepared according to a literature procedure.¹⁵ The occurrence of an NMR enantiodifferentiation and of a possible chiral recognition between the ionic species was then studied by ³¹P{¹H} NMR spectroscopy. A solution of [Mo₃S₄Cl₃(dppe)₃][Δ-TRISPHAT] was prepared in C₆D₆:CD₃CN (97:3).¹⁶ This solvent ratio ensures total solubilization of the cluster salt with the lowest solvent polarity. As expected, the hexacoordinated phosphate anion behaved as an NMR chiral solvating agent. Distinguishable signals for the diastereomeric homochiral [*P*-Mo₃S₄Cl₃(dppe)₃][Δ-TRISPHAT] and het-

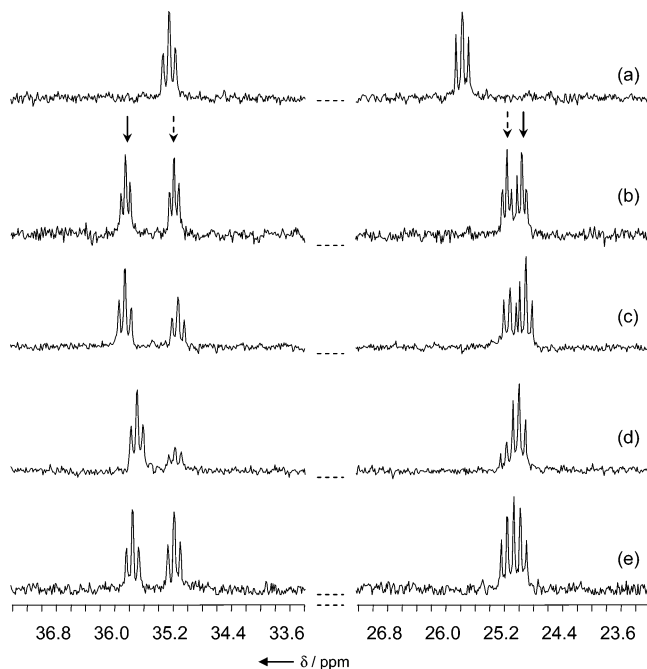


Figure 3. ³¹P{¹H} NMR spectra in C₆D₆:CD₃CN (97:3) of (a) racemic [Mo₃S₄Cl₃(dppe)₃][PF₆]⁻ and of [*rac*-Mo₃S₄Cl₃(dppe)₃][Δ-TRISPHAT] after (b) ion pairing exchange and (c) heating at 72 °C for 4 h. Filtrate (d) and precipitate (e) fractions obtained after leaving the 1.2:1 diastereomer ratio at 20 °C for 72 h.

erochiral [*M*-Mo₃S₄Cl₃(dppe)₃][Δ-TRISPHAT] salts were observed, as shown in Figure 3.¹⁷ Each of the two phosphorus signals in the [Mo₃S₄Cl₃(dppe)₃]⁺ cluster cation, corresponding to the phosphorus atoms located above and below the metal plane, are split into two signals. The ratio between the two diastereomeric ion pairs is 1:1 (Figure 3, spectrum b). Two hypotheses could then be considered to explain the above-described result: (i) a configurational stability for the [Mo₃S₄Cl₃(dppe)₃]⁺ cluster cation at room temperature or (ii) a configurational lability and a lack of a supramolecular stereocontrol from anion Δ-TRISPHAT over the geometry of the cationic cluster.

Asymmetric Induction of [Mo₃S₄Cl₃(dppe)₃]⁺ by Enantiopure TRISPHAT. To discriminate between these two hypotheses, the solution of [*rac*-Mo₃S₄Cl₃(dppe)₃][Δ-TRISPHAT] was heated at 72 °C for 4 h, and in sharp contrast to the situation at 20 °C, integration of the separated signals indicated an imbalance in the diastereomeric population and the predominance of one enantiomeric form of the cation over the other (diastereomeric ratio dr 1.2:1, Figure 3, spectrum c). Longer heating periods did not improve the diastereomeric ratio, which was also preserved upon cooling to room temperature. However, within minutes at 20 °C, crystals started forming which could be easily separated from the solution by filtration. The ³¹P{¹H} NMR spectra of the filtrate then showed an enrichment of the diastereomeric ratio that reached a decent 4:1 value after 72 h. Heating this resulting filtrate at 72 °C for 4 h led to the recovery of the

- (11) Yeh, R. M.; Raymond, K. N. *Inorg. Chem.* **2006**, *45*, 1130–1139. Vignon, S. A.; Wong, J.; Tseng, H.-R.; Stoddart, J. F. *Org. Lett.* **2004**, *6*, 1095–1098. Bonnot, C.; Chambron, J. C.; Espinosa, E. *J. Am. Chem. Soc.* **2004**, *126*, 11412–11413. Yeh, R. M.; Ziegler, M.; Johnson, D. W.; Terpin, A. J.; Raymond, K. N. *Inorg. Chem.* **2001**, *40*, 2216–2217. Owen, D. J.; VanDerveer, D.; Schuster, G. B. *J. Am. Chem. Soc.* **1998**, *120*, 1705–1717. Green, M. M.; Khatri, C.; Peterson, N. C. *J. Am. Chem. Soc.* **1993**, *115*, 4941–4942. Kirschner, S.; Ahmad, N.; Munir, C.; Pollock, R. J. *Pure Appl. Chem.* **1979**, *51*, 913–923. Norden, B.; Tjernerfeld, F. *FEBS Lett.* **1976**, *67*, 368–370. Pfeiffer, P.; Quehl, K. *Chem. Ber.* **1931**, *64*, 2667–2671.
- (12) Winkelmann, O.; Linder, D.; Lacour, J.; Näther, C.; Lüning, U. *Eur. J. Org. Chem.* **2007**, 3687–3697. Hebbe-Viton, V.; Desvergues, V.; Jodry, J. J.; Dietrich-Buchecker, C.; Sauvage, J.-P.; Lacour, J. *Dalton Trans.* **2006**, 2058–2065. Bergman, S. D.; Frantz, R.; Gut, D.; Kol, M.; Lacour, J. *Chem. Commun.* **2006**, 850–852. Vial, L.; Gonçalves, M.-H.; Morgantini, P.-Y.; Weber, J.; Bernardinelli, G.; Lacour, J. *Synlett* **2004**, 1565–1568. Martínez-Viviente, E.; Pregosin, P. S.; Vial, L.; Herse, C.; Lacour, J. *Chem. Eur. J.* **2004**, *10*, 2912–2918. Constable, E. C.; Frantz, R.; Housecroft, C. E.; Lacour, J.; Mahmood, A. *Inorg. Chem.* **2004**, *43*, 4817–4819. Hiraoka, S.; Harano, K.; Tanaka, T.; Shiro, M.; Shionoya, M. *Angew. Chem., Int. Ed.* **2003**, *42*, 5182–5185. Vial, L.; Lacour, J. *Org. Lett.* **2002**, *4*, 3939–3942. Pasquini, C.; Desvergues-Breuil, V.; Jodry, J. J.; Dalla Cort, A.; Lacour, J. *Tetrahedron Lett.* **2002**, *43*, 423–426. Monchaud, D.; Jodry, J. J.; Pomeranc, D.; Heitz, V.; Chambron, J.-C.; Sauvage, J.-P.; Lacour, J. *Angew. Chem., Int. Ed.* **2002**, *41*, 2317–2319. Lacour, J.; Jodry, J. J.; Monchaud, D. *Chem. Commun.* **2001**, 2302–2303. Lacour, J.; Jodry, J. J.; Ginglinger, C.; Torche-Haldimann, S. *Angew. Chem., Int. Ed.* **1998**, *37*, 2379–2380.
- (13) Jodry, J. J.; Frantz, R.; Lacour, J. *Inorg. Chem.* **2004**, *43*, 3329–3331.
- (14) Laleu, B.; Bernardinelli, G.; Chauvin, R.; Lacour, J. *J. Org. Chem.* **2006**, *71*, 7412–7416.
- (15) Lacour, J.; Barchéchath, S.; Jodry, J. J.; Ginglinger, C. *Tetrahedron Lett.* **1998**, *39*, 567–570.
- (16) A good balance between high polarity solvent conditions for solubility and a low polarity medium for effective enantiodifferentiation was provided by mixtures of CD₃CN (3–10%) in C₆D₆.

- (17) TRISPHAT anion is particularly effective for the recognition of cationic bisaryl or trisaryl phosphorus derivatives. See refs 10 and 13 and Hebbe, V.; Londez, A.; Goujon-Ginglinger, C.; Meyer, F.; Uziel, J.; Jugé, S.; Lacour, J. *Tetrahedron Lett.* **2003**, *44*, 2467–2471.

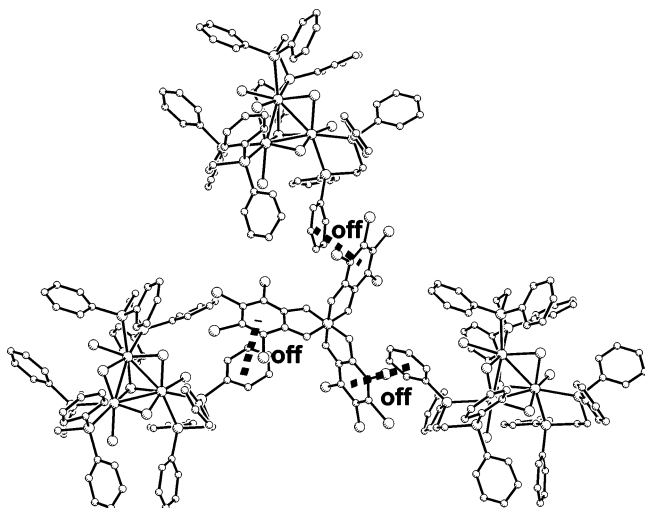


Figure 4. Homochiral P - Δ interactions in racemic $[\text{Mo}_3\text{S}_4\text{Cl}_3(\text{dppe})_3]$ (TRISPHAT). Offset face-to-face (off) interactions are marked as dashed lines.

original 1.2:1 ratio.¹⁸ With these results in hand, only the first hypothesis that considers a configurational stability of the cluster cation at 20 °C (and a lability at elevated temperature) is plausible.

The crystal structure of the precipitate was determined by single-crystal X-ray diffraction. To our initial surprise, the solid crystallizes in the centrosymmetric $P\bar{1}$ space group, and therefore, racemization of the TRISPHAT anion must have occurred to some extent. Interatomic bond distances within the $[\text{Mo}_3\text{S}_4\text{Cl}_3(\text{dppe})_3]^+$ cluster are similar to those observed for closely related complexes.² Structural motifs occurring in the crystal presents homochiral P - Δ and M - Δ interactions in which each anion is surrounded by three homochiral cluster cations, as represented in Figure 4. The main interactions within these motifs, other than electrostatic interactions, are those derived from contacts between phenyl groups. Three types of pairwise phenyl–phenyl configurations are recognized, namely, offset face-to-face (off) (marked as dashed lines) and several edge-to-face (ef) and vertex-to-face (vf) (according to the nomenclature introduced by Dance);¹⁹ however, the importance of this homochiral supramolecular motif in solution is debatable (vide infra, next section). A circular dichroism (CD) analysis of the precipitate was also performed and showed a complete lack of Cotton effects in the spectral region in which the cluster cation absorbs, confirming that the racemic crystal employed in the diffraction experiments was representative of the bulk precipitate sample.

Global Explanation and Sense of Induction. At this stage, several points seemed to be clearly established: (i) the configurational stability of the $[\text{Mo}_3\text{S}_4\text{Cl}_3(\text{dppe})_3]^+$ cation

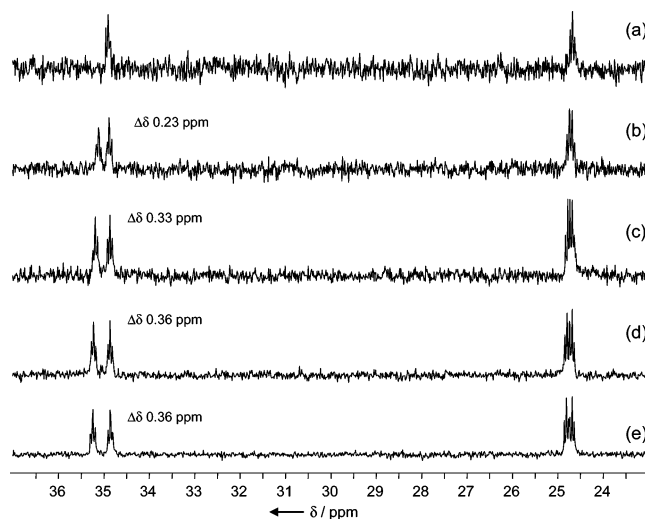


Figure 5. $^{31}\text{P}\{^1\text{H}\}$ NMR spectra in $\text{C}_6\text{D}_6:\text{CD}_3\text{CN}$ (95:5) of $[\text{rac}\text{-Mo}_3\text{S}_4\text{Cl}_3(\text{dppe})_3][\text{PF}_6]$ after the addition of (a) 0.0, (b) 0.1, (c) 0.2, (d) 0.3, and (e) 0.4 equiv of $[\text{nBu}_4\text{N}][\Delta\text{-TRISPHAT}]$.

at room temperature, (ii) its lability at higher temperature (e.g., 72 °C), (iii) the subsequent stereocontrol of Δ -TRISPHAT anion on the equilibrating diastereomers at elevated temperature (dr 1.2:1), and (iv) a racemization of the Δ -TRISPHAT anion at elevated temperature, leading, upon lowering of the temperature,²⁰ to the precipitation of $[\text{rac}\text{-Mo}_3\text{S}_4\text{Cl}_3(\text{dppe})_3]$ - $[\text{rac}\text{-TRISPHAT}]$ and causing an increase in the diastereomeric ratio in solution (dr up to 4:1) by depleting more strongly from solution the minor stereoisomer of $[P\text{-Mo}_3\text{S}_4\text{Cl}_3(\text{dppe})_3]$ and $[M\text{-Mo}_3\text{S}_4\text{Cl}_3(\text{dppe})_3]$ over the other.

However, one experiment seemed to contradict this explanation. The $^{31}\text{P}\{^1\text{H}\}$ NMR spectrum of the precipitate in $\text{C}_6\text{D}_6:\text{CD}_3\text{CN}$ (95:5) that still showed an enantiodifferentiation of the signals of the P and M enantiomers of the chiral cationic cluster with a separation of the signals essentially as large ($\Delta\delta$ 0.68 ppm, 1:1 ratio) as that observed for the initial $[\text{rac}\text{-Mo}_3\text{S}_4\text{Cl}_3(\text{dppe})_3][\Delta\text{-TRISPHAT}]$ salt in essentially the same solvent conditions (Figure 3, spectrum b); this observation is in apparent contradiction with the previous explanation advocating for the presence of only racemic TRISPHAT in the precipitate.

This apparently paradoxical NMR behavior could then be explained by an NMR titration experiment. Various amounts of $[\text{nBu}_4\text{N}][\Delta\text{-TRISPHAT}]$ were added in small portions to a solution of racemic $[\text{Mo}_3\text{S}_4\text{Cl}_3(\text{dppe})_3][\text{PF}_6]$ in $\text{C}_6\text{D}_6:\text{CD}_3\text{CN}$ (95:5). The different spectra are reported in Figure 5. Very small amounts of the Δ -TRISPHAT salt are sufficient to induce the enantiodifferentiation—as low as 0.1 equiv and leading a decent separation ($\Delta\delta$ 0.23 ppm). More surprisingly, 0.3 equiv of Δ -TRISPHAT is sufficient to achieve the maximal NMR split efficiency ($\Delta\delta_{\text{max}}$ 0.36 ppm), any further addition of $[\text{nBu}_4\text{N}][\Delta\text{-TRISPHAT}]$ leading to no further modifications of the NMR spectra. This clearly indicates that the enantiodifferentiation of the chiral cationic cluster by Δ -TRISPHAT reaches a plateau at very low stoichiometry. As such, any small amount of $[\text{rac}\text{-Mo}_3\text{S}_4\text{Cl}_3(\text{dppe})_3][\Delta\text{-TRISPHAT}]$ salt is sufficient to induce the enantiodifferentiation of the chiral cationic cluster.

(18) From the latter experiment, a maximum value for the energy barrier of enantiomerization of the cluster cation can be estimated. Assuming that it takes 10 half-lives to reach equilibrium, the maximum half-life for the enantiomerization can be estimated as 24 min at 72 °C. This in turn corresponds to an upper limit for the energy of enantiomerization of 25.5 kcal/mol.

(19) Scudder, M.; Dance, I. *J. Chem. Soc., Dalton Trans.* **1998**, 329–344. Dance, I.; Scudder, M. *Chem. Eur. J.* **1996**, *2*, 481–486. Dance, I.; Scudder, M. *J. Chem. Soc., Chem. Comm.* **1995**, 1039–1040.

(20) At room temperature, chiroptical characterization of the mother liquor indicates a lack of further racemization of TRISPHAT anion.

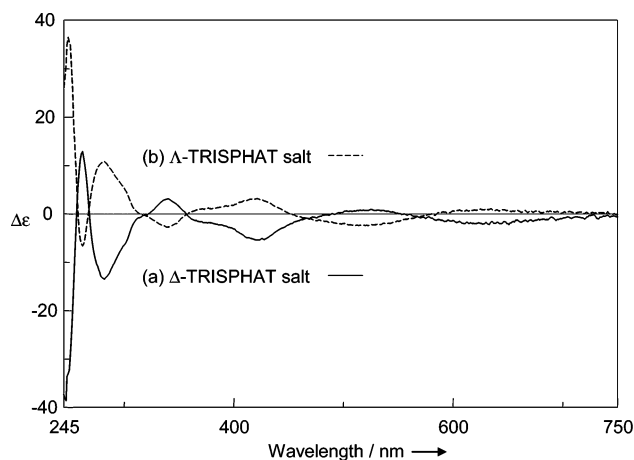


Figure 6. CD spectra of the filtrate fractions resulting from association of $[\text{Mo}_3\text{S}_4\text{Cl}_3(\text{dppe})_3]^+$ with (a) Δ -TRISPHAT (—) and (b) Λ -TRISPHAT (---).

$\text{Cl}_3(\text{dppe})_3][\Delta\text{-TRISPHAT}]$ salt “contaminating” the precipitate fraction will produce the observed split of the ^{31}P NMR signals; this contamination most probably occurs at the filtration stage of the protocol.

Finally, one important stereochemical issue remained and concerned the nature of preferred configuration of the cationic cluster after equilibration in the presence of TRISPHAT. For this determination, solutions of $[\text{rac-Mo}_3\text{S}_4\text{Cl}_3(\text{dppe})_3][\Delta\text{-TRISPHAT}]$ and $[\text{rac-Mo}_3\text{S}_4\text{Cl}_3(\text{dppe})_3][\Lambda\text{-TRISPHAT}]$ in $\text{C}_6\text{D}_6\text{:CD}_3\text{CN}$ (95:5) were heated at 72 °C for 24 h and allowed to cool down to room temperature for 24 h. After filtration and NMR characterization, the CD spectra of the filtrates were recorded (see Figure 6). As expected, equal and opposite Cotton effects were observed for the spectra issued from the Δ - and Λ -TRISPHAT salts in the characteristic region of the cluster’s centered d–d absorption bands, around 270 and 420 nm.²¹ These spectra were assigned to cationic cluster complexes of M and P configurations, respectively. The assignment was done by comparison with the CD spectra of the previously reported $[\text{P-Mo}_3\text{S}_4\text{Cl}_3((R,R)\text{-Me-BPE})_3]^+$ and $[\text{M-Mo}_3\text{S}_4\text{Cl}_3((S,S)\text{-Me-BPE})_3]^+$ cluster enantiomers.⁴ Interestingly, and a bit surprisingly, the association of enantiopure TRISPHAT anions with racemic $[\text{Mo}_3\text{S}_4\text{Cl}_3(\text{dppe})_3]^+$ clusters leads at elevated temperature and in nonpolar conditions to a stereoselective induction in favor of the heterochiral ($M^+ \Delta^-$ or $P^+ \Lambda^-$) rather than the “classical” homochiral association; the origin of this reversal of the traditional trend is the subject of further investigations.²²

Theoretical Investigation on the $[\text{P-Mo}_3\text{S}_4\text{Cl}_3(\text{dppe})_3]^+$ and $[\text{M-Mo}_3\text{S}_4\text{Cl}_3(\text{dppe})_3]^+$ Interconversion. The origin of the TRISPHAT racemization remained however somewhat mysterious. The most logical explanation was the partial decomplexation of one diphosphane ligand at elevated

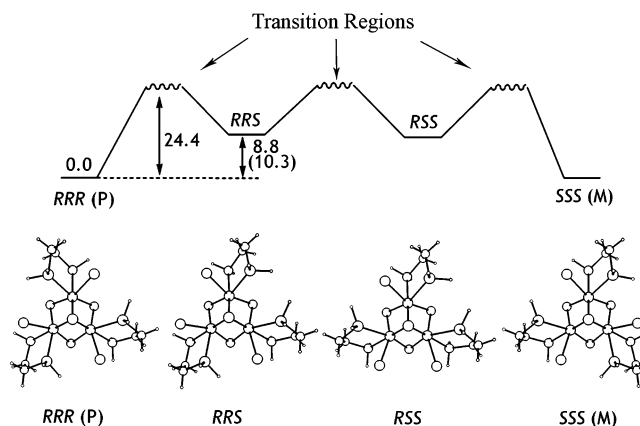


Figure 7. Proposed stepwise mechanism for the transformation of $[\text{P-Mo}_3\text{S}_4\text{Cl}_3(\text{diphosphane})_3]^+$ into $[\text{M-Mo}_3\text{S}_4\text{Cl}_3(\text{diphosphane})_3]^+$, with relative energies (in kcal/mol) calculated by QM and QM/MM (in parenthesis) methods. QM-optimized geometries for the model system are plotted below.

temperature, creating a Lewis acidic site, this electron-poor metal center being able to interact with one of the oxygen atoms of the TRISPHAT anion and induce the acid-catalyzed racemization pathway.⁶ In order to validate this hypothesis, theoretical calculations on the $[\text{P-Mo}_3\text{S}_4\text{Cl}_3(\text{diphosphane})_3]^+ \leftrightarrow [\text{M-Mo}_3\text{S}_4\text{Cl}_3(\text{diphosphane})_3]^+$ interconversion mechanism were carried out using quantum mechanical (QM) and hybrid quantum and molecular mechanical (QM/MM) methodologies as described in the following section.

Due to the size and complexity of the system, two approximations have been taken into account for pure QM calculations: the counterion is not included in the model and the diphosphane phenyl groups have been replaced by hydrogen atoms. Steric repulsions between phenyl groups for these congested structures have been evaluated through QM/MM calculations. The energy profile for the less energetically demanding mechanism for the interconversion of $[\text{P-Mo}_3\text{S}_4\text{Cl}_3(\text{dppe})_3]^+$ into $[\text{M-Mo}_3\text{S}_4\text{Cl}_3(\text{dppe})_3]^+$ is depicted in Figure 7, where each of the Mo centers rearranges the Cl and diphosphane ligands sequentially: $RRR (P) \rightarrow RRS \rightarrow RSS \rightarrow SSS (M)$. The R and S refer to the configuration around the octahedral environment of the metal atoms. Intermediates (RRS and RSS) have been optimized using BP86/VPTZ methodologies and characterized as minima in the potential energy surface, lying 8.8 kcal/mol higher in energy than the P and M configurations. Intermediates are connected through transition state regions, as we will see later on in this section.

The first intermediate in this three-step reaction mechanism corresponds to the RRS structure with two hydrogen atoms in equatorial positions facing each other at an interatomic distance of 2.245 Å. Replacement of the phosphorus hydrogen atoms by phenyl groups increases the difference between the RRS intermediate and the $RRR (P)$ starting cluster cation only to 10.3 kcal/mol, due to the flexibility of the diphosphane ligand to accommodate the phenyl groups; in consequence, steric hindrance coming from the bulkier $-\text{Ph}$ groups does not hamper the proposed reaction pathway. A detailed analysis of the topology of the PES in the region between $RRR (P)$ and RRS reveals that they are not connected

(21) TRISPHAT chromophores absorb under 270 nm, see: Bas, D.; Bürgi, T.; Lacour, J.; Vachon, J.; Weber, J. *Chirality* **2005**, *17*, S143–S148. All Cotton effects observed above this threshold are those of the nonracemic cationic complexes.

(22) Preferred heterochiral associations have already been observed in the presence of TRISPHAT anions either in solution or in the solid state. See refs 13 and 14.

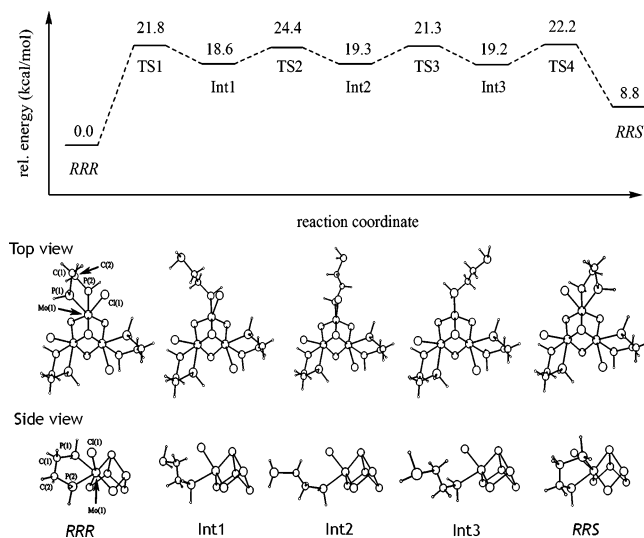


Figure 8. DFT relative energies (in kcal/mol) for the proposed reaction mechanism along the first TSs region. The optimized geometries are plotted below (top view for all atoms and side view for selected atoms).

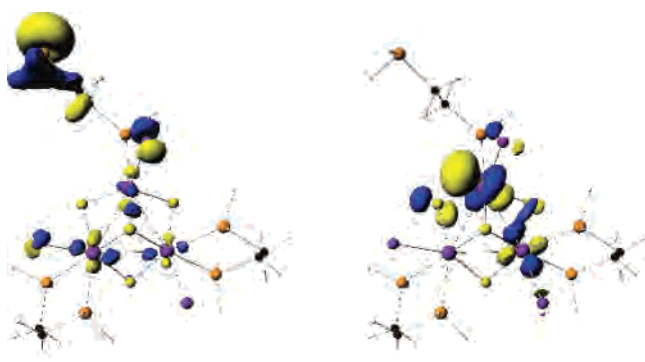


Figure 9. BP86/VTZP HOMO (left) (-0.3095 au) and LUMO+3 (right) (-0.2330 au) orbitals for Int1 depicted at the 0.05 contour level.

through a single transition state (TS) but by a so-called TSs region (see Figure 8). Decoordination from the metal, Mo(1), of one phosphorus atom of the diphosphane ligand, namely the one trans to the bridging sulfur, P(1), allows the rotation of C(1)–C(2), C(1)–P(1), and Mo(1)–P(1) single bonds across low-energy barriers, leading to manifold stable conformations. The TSs region is concluded by the formation of the Mo(1)–P(1) dative bond reaching intermediate RRS.

A suitable guiding reaction coordinate for the first step of the interconversion mechanism is the rotation of the PH_2 group around the C(1)–C(2) bond (see Figure 8), from 50.0° in RRR to 116.4° at the transition state (TS1) and 196° at the first reaction intermediate (Int1). The TS1 presents a very low imaginary frequency of -76.1 cm^{-1} associated with the twisting of the dihedral P(2)–C(2)–C(1)–P(1) angle. The BP86/VTZP calculated activation and reaction energies are 21.8 and 18.6 kcal/mol, respectively. Figure 9 shows the HOMO and LUMO+3 orbitals of the Int1 structure. The HOMO orbital corresponds to the P(1) atom lone pair, while the major contribution to the LUMO+3 orbital comes from Mo(1) d_{z^2} empty orbital, which can act as a Lewis acid site for the catalysis of the TRISPHAT racemization, as experimentally observed. A detailed computational investigation

on this process is being carried out in our laboratory, and the results will be presented in due course.

Once the diphosphane ligand is bonded to the molybdenum atom just by the Mo(1)–P(2) bond, the Cl(1) atom can move to a position intermediate between that for RRR and RRS. The coordination environment around Mo(1) is now a trigonal bipyramid. The rotation around C–C and C–P single bonds takes place via very low-energy barrier, leading to Int3, which corresponds to the mirror image of Int1. Finally, the first step of the interconversion mechanism concludes by the formation of a dative bond between the P(1) lone pair and an empty d_{z^2} orbital on Mo(1), reaching RRS. The same mechanistic picture can be drawn for the other two transition regions associated with the remaining metal atoms of the triangular cluster. Therefore, the highest energy barrier for the interconversion of the RRR configuration in $[P\text{-Mo}_3\text{S}_4\text{Cl}_3(\text{diphosphane})_3]^+$ into the SSS configuration in $[M\text{-Mo}_3\text{S}_4\text{Cl}_3(\text{diphosphane})_3]^+$ is 24.4 kcal/mol. This value explains that asymmetric induction of $[P\text{-Mo}_3\text{S}_4\text{Cl}_3(\text{diphosphane})_3]^+$ by the optically pure anion $\Delta\text{-TRISPHAT}$ is only observed at elevated temperatures.

Conclusion

Experimental data indicate that C_3 -symmetric cationic clusters of type $[\text{Mo}_3\text{S}_4\text{Cl}_3(\text{dppe})_3]^+$ are configurationally stable at 20°C and somewhat labile at elevated temperature—a property unknown to this point. At 72°C , an equilibrium between the *P* and *M* enantiomers of the cluster could be evidenced and used to induce, in the presence of TRISPHAT anion, an unbalance among the diastereomeric salts. The moderate but definite diastereoselectivity (1.2:1) obtained at elevated temperature can be increased by the in-situ precipitation at room temperature of the racemic $[\text{Mo}_3\text{S}_4\text{Cl}_3(\text{dppe})_3][\text{TRISPHAT}]$ salt that improves the diastereomeric purity of the mother liquor to 4:1 ratio. Interestingly, the preferred association of the chiral three-bladed propeller in solution at 72°C is of heterochiral ($M^+ \Delta^-$ or $P^+ \Lambda^-$) rather than homochiral nature.

Experimental Section

General. $^{31}\text{P}\{^1\text{H}\}$ NMR spectra were recorded on Bruker AMX-400 MHz spectrometer, using $\text{C}_6\text{D}_6\text{:CD}_3\text{CN}$ (95:5) as a solvent, and are referenced to external 85% H_3PO_4 . Electrospray ionization (ESI) mass spectra were recorded on a Quattro LC mass spectrometer using CH_2Cl_2 as solvent. Circular dichroism measurements were recorded on a JASCO J-810 spectrometer. The sample solutions were prepared in a quartz cuvette of 1 cm path length and measured at 25°C . All halogenated solvents were filtered over basic alumina before use.

Preparation of Compounds. $[\text{Mo}_3\text{S}_4(\text{dppe})_3\text{Cl}_3](\text{PF}_6)$, [cinchonidinium][$\Delta\text{-TRISPHAT}$], and $[^n\text{Bu}_3\text{NH}][\Lambda\text{-TRISPHAT}]$ were prepared following literature procedures.

Association of $[\text{Mo}_3\text{S}_4(\text{dppe})_3\text{Cl}_3]^+$ with TRISPHAT. To a solution of 120 mg of $[\text{Mo}_3\text{S}_4(\text{dppe})_3\text{Cl}_3][\text{PF}_6]$ in dichloromethane was added a saturated solution of 68 mg of [cinchonidinium][$\Delta\text{-TRISPHAT}$] in acetone. The resulting mixture was stirred for 5 min, concentrated in vacuo, dissolved in the minimum amount of dichloromethane, and charged onto a silica gel column. The green band that eluted contained the desired product, which was dried

under vacuum overnight to afford 110 mg of [*rac*-Mo₃S₄(dppe)₃-Cl₃][Δ-TRISPHAT] (yield 69%). ³¹P{¹H} NMR (121.47 MHz, C₆D₆:CD₃CN (95:5), 25 °C): δ = -79.9 (s), 25.0 (t), 25.2 (t) 35.3 (t), 35.9 ppm (t). UV/vis (CHCl₃): λ_{max} (ε) = 408 (6827.60), 299 nm (14 165.52 mol⁻¹ dm³ cm⁻¹). ESI-MS (30 V): *m/z* (%) 1723 (100) [M⁺]. The association with Δ-TRISPHAT was carried out following the same procedure but using 80 mg of cluster and 41 mg of [Bu₃NH][Δ-TRISPHAT], yielding 75 mg of [*rac*-Mo₃S₄(dppe)₃Cl₃][Δ-TRISPHAT] (yield 70%).

Asymmetric Induction: Salt [*rac*-Mo₃S₄(dppe)₃Cl₃][Δ-TRISPHAT] or [*rac*-Mo₃S₄(dppe)₃Cl₃][Λ-TRISPHAT] (25 mg) was dissolved in 700 μL of C₆D₆:CD₃CN (95:5). The solution was heated at 72 °C for 4–36 h and allowed to cool to room temperature. Within the next hour, green crystals started forming, and 72 h later they were separated from the solution by filtration, washed with cold benzene, and dried with pentane (17 mg, 68%). Characterization data for the precipitate and the filtrate fractions are essentially identical to the ones described in the previous paragraph, except for the CD spectra and the relative intensities of the ³¹P{¹H} NMR signals.

Microtitration. [Bu₄N][Δ-TRISPHAT] (0.1 equiv, 5 μL, 0.82 mg, 0.81 μmol) in 25.2 μL of a mixture of C₆D₆:CD₃CN (95:5) was added stepwise to a solution of [Mo₃S₄(dppe)₃Cl₃][PF₆] (3 mg, 1.61 μmol) in 700 μL of C₆D₆:CD₃CN (95:5) and a NMR spectrum was recorded after each addition. The spectra are shown in Figure 7.

X-ray Data Collection and Structure Refinement. X-ray diffraction experiments were carried out on a Bruker SMART CCD diffractometer using Mo Kα radiation (λ = 0.710 73 Å) at room temperature. The data were collected with a frame width of 0.3° in ω at a crystal to detector distance of 4 cm. The diffraction frames were integrated using the SAINT package and corrected for absorption with SADABS.²³ The structures were solved by direct methods and refined by the full-matrix method based on *F*² using the SHELXTL software package.²⁴ Difference Fourier maps were done to locate the remaining atoms. Refinement was performed by the full-matrix-least-square method based on *F*². All atoms in the anion and the cluster cation except one phenyl group [C(59) to C(64)] were refined anisotropically. This group had to be refined isotropically with a fixed geometry. Hydrogen atoms were generated geometrically, assigned isotropic thermal parameters, and allowed to ride on their respective parent C atoms. Three independent benzene crystallization molecules [C(900) to C(905), C(906) to C(911), and C(912) to C(917)] were found and refined isotropically with 1, 0.5, and 0.5 occupancies, respectively. A fourth independent benzene molecule appeared defined only by three carbon [C(918) to C(920)] atoms related through an inversion center. Crystal data for [Mo₃S₄(dppe)₃Cl₃](TRISPHAT): C₁₁₁H₉₃C₁₁₅Mo₃O₆P₇S₄, *M* = 2687.45, triclinic, space group *P* $\bar{1}$, *a* = 17.1206(14) Å, *b* = 19.6851(15) Å, *c* = 20.7160(16) Å, α = 97.010(2)°, β = 92.467(2)°, γ = 108.341(2)°, *V* = 6552.9(9) Å³, *T* = 293 K, *Z* = 2, μ(Mo Kα) = 0.784 mm⁻¹, reflections collected/unique = 36 895/22 938 (*R*_{int} = 0.0676), final refinement converged with *R*₁ = 0.0806 for 11 349 reflections with *F*₀ ≥ 4σ(*F*₀) and *wR*₂ = 0.2615 for all reflections, *GOF* = 1.178, max/min residual electron density 1.174 and -1.030 e⁻Å⁻³.

Computational Details. All theoretical calculations were carried out with the ADF 2005 program.²⁵ Molecular orbitals were

expanded using uncontracted double-ζ and one polarization Slater basis sets. Large frozen cores (Mo4p, Cl2p, S2p, P2p, C1s) were employed for heavy atoms. An auxiliary set of s, p, d, f, and g STOs was used to fit the molecular density and to represent the Coulomb and exchange potentials accurately in each SCF cycle.

We used the local spin density approximation, characterized by the electron gas exchange (Xa with *x* = 2/3) together with Vosko–Wild–Nusair parametrization²⁶ for correlation. Becke's nonlocal correction²⁷ to the exchange energy and Perdew's nonlocal corrections²⁸ to the correlation energy was added. Geometries were optimized using analytical gradient techniques until the maximum gradient component was less than 1.0 × 10⁻⁴ au. Vibrational frequencies were obtained through numerical differentiation of the analytical gradients. Scalar relativistic corrections were included self-consistently by means of the zeroth-order regular approximation (ZORA)²⁹ using corrected core potentials. The quasirelativistic frozen core shells were generated with the auxiliary program DIRAC.

Hybrid QM/MM calculations were carried out using the a modified version³⁰ of the original IMOMM scheme developed by Morokuma and Maseras.³¹ The QM part is treated at the same level as pure DFT calculations (BP86/VDZP), while the MM part is calculated using the Sybyl force field.³²

Acknowledgment. The financial support of the Spanish Ministerio de Educación y Ciencia (MEC) and the EU FEDER Program (Grants BQU2002-00313 and CTQ2005-09270-C02-01), Fundació Bancaixa-UJI (research project P1.1B2004-19), and Generalitat Valenciana (research projects ACOMP/2007/286) is gratefully acknowledged. The authors also thank the Servei Central D'Instrumentació Científica (SCIC) of the Universitat Jaume I for providing us with spectroscopic and X-ray facilities. V.P. thanks support from the Juan de la Cierva fellowship from the MEC. We are also grateful for financial support of this work by the Swiss National Science Foundation, the Federal Office for Education and Science and the Sandoz Family Foundation (R.F., J.L.).

Supporting Information Available: X-ray crystallographic file in CIF format, and energy and geometrical data for all structures theoretically calculated. This material is available free of charge via the Internet at <http://pubs.acs.org>.

IC701522P

(23) SAINT, 5.0 ed.; Bruker Analytical X-ray Systems; Madison, WI, 1996. Sheldrick, G. M. *SADABS empirical absorption program*; University of Göttingen, 1996.

(24) Sheldrick, G. M. *SHELXTL*, 5.1 ed.; Bruker Analytical X-ray Systems; Madison, WI, 1997.

(25) Velde, G. T.; Bickelhaupt, F. M.; Baerends, E. J.; Guerra, C. F.; Van Gisbergen, S. J. A.; Snijders, J. G.; Ziegler, T. *J. Comp. Chem.* **2001**, *22*, 931–967.

(26) Vosko, S. H.; Wilk, L.; Nusair, M. *Can. J. Phys.* **1980**, *58*, 1200–1211.

(27) Becke, A. D. *Phys. Rev. A* **1988**, *38*, 3098–3100.

(28) Perdew, J. P. *Phys. Rev. B* **1986**, *33*, 8822–8824. Perdew, J. P. *Phys. Rev. B* **1986**, *34*, 7406–7406.

(29) Vanlenthe, E.; Baerends, E. J.; Snijders, J. G. *J. Chem. Phys.* **1993**, *99*, 4597–4610.

(30) Woo, T. K.; Cavallo, L.; Ziegler, T. *Theor. Chem. Acc.* **1998**, *100*, 307–313.

(31) Maseras, F.; Morokuma, K. *J. Comput. Chem.* **1995**, *16*, 1170–1179.

(32) Clark, M.; Cramer, R. D.; Vanopdenbosch, N. *J. Comput. Chem.* **1989**, *10*, 982–1012.